



Microplastics formation based on degradation characteristics of beached plastic bags

P. Tziourrou^a, S. Kordella^b, Y. Ardali^c, G. Papatheodorou^b, H.K. Karapanagioti^{a,*}

^a Department of Chemistry, University of Patras, Patras, Greece

^b Laboratory of Marine Geology and Physical Oceanography, Department of Geology, University of Patras, Patras, Greece

^c Department of Environmental Engineering, Ondokuz Mayıs University, Samsun, Turkey

ARTICLE INFO

Keywords:

Plastic bags
Microplastics
Marine pollution
Coastal zone
Fragmentation

ABSTRACT

Environmental pollution from plastic bags is a significant issue in the global environment. Plastic bags can be transferred by the wind and ocean currents everywhere in the three dimensions and be fragmented into small particles, termed film-shaped microplastics. The purpose of this study is to provide insights on the degradation of beached plastic bags. Monitoring and sampling were performed to determine plastic bag fragmentation and the possible mechanisms. On selected samples, various spectroscopic techniques and microscopy were used. Before the imposition of the "green" plastic bag fee in Greece, field monitoring suggested that the majority of the coastal plastic bags were fragmented whereas after the "green" fee, less fragmented bags were observed. Evidence of three degradation mechanisms were observed in this study. For oxodegradable plastic bags, degradation takes place for the starch additives and the polymer part stays in the environment as microplastic particles. For thin light density polyethylene plastic bags, mechanical fragmentation takes place in the environment creating microplastics before significant chemical alterations in functional groups were observed and once chemical alteration (oxidation) is observed, fragmentation (of H—C or C—C bonds) is also taking place. Thus, regulating thin plastic bags usage removes problems related to plastic bags but also to film-shaped microplastics.

1. Introduction

Shopping bags are strong, cheap, and lightweight plastic items, hence, are used widely in global scale (Saidan et al., 2017). They were introduced in 1970s, but currently ~500 billion [which can reach up to 5 trillion (Knoblauch et al., 2018)] plastic bags are used per year internationally (Moharam and Almaqtari, 2014). Non-renewable resources, such as petroleum and natural gas, are used as raw materials (Saidan et al., 2017) from which only 5% or less are recycled worldwide (Knoblauch et al., 2018). Measures against plastic bag use could play a more effective role than recycling in the battle against marine plastic bag pollution. Maes et al. (2018) suggested that such measures could be the reasons for downward trends in plastic bag accumulations on the seafloor around the UK's coastline.

To date, marine pollution by single use plastic bags is poorly investigated. Polyethylene [e.g., Low Density Polyethylene (LDPE)] is a common material of shopping bags (Balestri et al., 2017), which is usually observed in different environments (e.g., coastal zones, global ocean, terrestrial ecosystems) with various ecological consequences.

Plastic bags, i.e., macroplastics (>5 mm) (Rummel et al., 2017), are commonly found marine debris (Clemente et al., 2018) and targeted environmental studies must be conducted, due to threatening marine and non-marine (e.g., human) species (Green et al., 2015; Clemente et al., 2018). Plastic pollution is known to travel throughout the world's oceans by winds and surface currents (Eriksen et al., 2014). Disposable plastic bags have recently been detected at 10,898 m depth; the deepest point of our planet (Mariana Trench, Western North Pacific) (Chiba et al., 2018), an important indication of plastic bags abundance in aquatic ecosystems.

Nevertheless, carrier bags were reported to degrade under environmental conditions including pressures such as solar radiation, oxidation (Nauendorf et al., 2016), microbial activity (biofilm) (Rummel et al., 2017), physical forces (e.g., sea waves) and also to fragment into smaller particles, so-called microplastics (<5 mm) (Rummel et al., 2017; Zhang, 2017). According to Kalogerakis et al. (2017), macroplastic debris should be collected on a regular basis from coastal zones before they are affected by weather conditions and thus, return to the marine environment as microplastics which travel everywhere with the wind since we

* Corresponding author.

E-mail address: karapanagioti@upatras.gr (H.K. Karapanagioti).




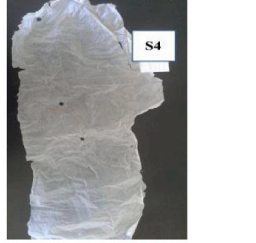



<https://doi.org/10.1016/j.marpolbul.2021.112470>

Received 2 March 2021; Received in revised form 6 April 2021; Accepted 7 May 2021

Available online 25 May 2021

0025-326X/© 2021 Elsevier Ltd. All rights reserved.

Table 1
Samples with their codes.

<i>Oxo-degradable plastic bags</i>		<i>Polyethylene plastic bags</i>	
Code of the sample	Photograph of the sample	Code of the sample	Photograph of the sample
S1		S3	
S2		S4	
Oxo-degradable P.B (microplastics)		S5	
-	-	S6	

are unable to collect them.

Existing sampling protocols for microplastics include a separate category of microplastics defined as films (Viršek et al., 2016; Masura et al., 2015; JRC, 2013). Some of these film-shaped microplastics possibly originate from plastic bags (northern Gulf of Mexico, Wessel et al., 2016; Corfu, Greece, Digka et al., 2018). Finally, microplastics can be detected in freshwater environments, such as Atoyac River basin (Mexico), where the film-shaped microplastics have been found in relatively significant abundance (Shruti et al., 2019).

In this study, an interdisciplinary approach is employed including field monitoring and laboratory analytical techniques to analyze and examine beached plastic bags, collected from Syros Island coastal zone, Greece. The objectives of the present study are the use of monitoring, spectroscopic techniques, and microphotographs to understand the degradation behaviour of the plastic bags in the coastal environment.

The goal is to better understand and provide insights to prevent the formation of microplastics from plastic bags.

2. Materials and methods

2.1. Sampling

In this study, the results of shredded versus intact plastic bags from 3 selected coastal sites (2 beaches and 1 harbour) of Syros Island, Aegean, Greece will be presented. The data was collected in 8 beach litter surveys spread over a 21-month period (May 2017–January 2019) in the framework of LIFE DEBAG project. The surveys included removal and classification of all beach stranded litter according to the MSFD protocol for marine litter monitoring in the European seas (Galvani et al., 2013). The protocol was modified so as to ensure the detailed monitoring of

beach stranded plastic bags in two points. Firstly, littered plastic bags were classified in 11 different categories based on their type and purpose, such as super-market/grocery shop bags, retail shop bags, garbage bags, polybags, oxo-degradable bags, etc. Secondly, the whole beach area was surveyed rather than a 50 or 100 m section that is proposed by the MSFD protocol. In this way, it is ensured that plastic bags, which have particular properties, and hence specific deposition sites on the beach depending on the hydro-dynamic regime and different meteorological conditions, were included in each survey if present in the total site area. What is more, it was distinguished in the records whether the beach stranded bag was shredded or not. In this study, the percentages of shredded supermarket/grocery shop (15–50 μm thick) and retail shop (thicker than 50 μm) plastic bags were considered, since these were the types of the collected samples.

During a sampling episode in May 2017 several plastic bags (35) were collected from Ladopoulos Beach. Based on their variable degradation state, six carrier bags (S1–6) were chosen by visual macroscopic observation for further characterization, were encoded i.e., non-degraded (S1 and S2), slightly degraded (S3 and S6), and highly degraded (S4 and S5), and were photographed (Table 1). No temperature effects such as air and water temperature are taken into consideration in this study. Additionally, an oxo-degradable plastic bag (P.B.) was placed in a dark box for a 3-year period to fragment into microplastics and a virgin low density polyethylene bag was used as blank sample.

2.2. Scanning Electron Microscopy (SEM)

Scanning Electron Microscopy (model JEOL 6300 of JEOL Company) was used to visually observe the surface topography and possible microbial colonization. The samples were spattered with Au using the MED 020 model of the BALTEC Company with being washed with deionized water.

2.3. Raman and Attenuated Total Reflectance - Fourier Transform Infrared Spectroscopy (ATR-FTIR) analysis

To identify the type and quality of chemical bonds, confocal Raman spectroscopy was used to analyze pieces of the plastic bags that their surface was not washed. A LabRAM HR800 (Horiba Jobin Yvon) spectrometer, equipped with a 488 nm laser and a 600 grooves/mm diffraction grating were used. The detector entrance slit was opened to 100 μm width. Samples were excited over 3 integration cycles of 10 s duration each. The incident beams were focused onto the samples through a 100 \times magnification objective. Multiple points were analyzed of each sample to check for spatial heterogeneity. Sample alteration was determined based on inter-comparison of Raman shifts and full width at half maximum intensities (FWHM) of characteristic Raman peaks. The profile parameters were determined by applying a profile fitting routine using LabSpec 6.0 (Horiba Jobin Yvon). The measurement range was 200–4000 cm^{-1} Raman shifts.

Attenuated Total Reflectance - Fourier Transform Infrared Spectroscopy (ATR - FTIR) was used to identify functional groups onto the samples. The spectra were obtained by "Bruker Optics' Alpha-P Diamond ATR Spectrometer of Bruker Optics GmbH" in 4000–400 cm^{-1} measurement range (resolution: 4 cm^{-1} , scans: 24). Before measurements all samples were wiped with a wet paper towel.

2.4. Diffuse Reflectance Spectroscopy (DRS)

The purpose of this technique was to identify electron transition in UV region and probable characterization of the samples in the visible

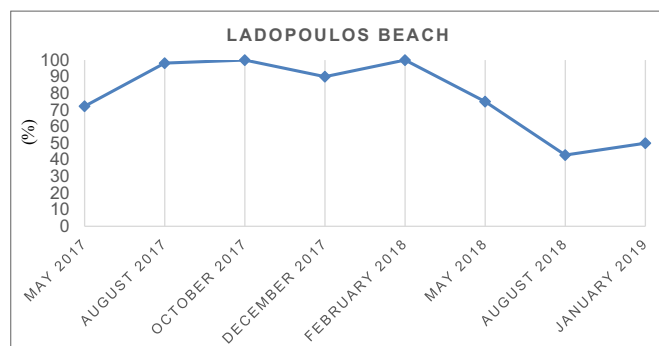


Fig. 1. Temporal variation of shredded plastic bag percentage in the most heavily polluted site: Ladopoulos Beach.

region of the DR spectra. Following a similar procedure as Tziourrou et al. (2020), UV-Vis spectrophotometer Varian Cary 3 was used. The blank of the instrument (PTFE reference disc) was used to calibrate and record spectra against the plastic bag samples in 200–800 nm region.

3. Results

3.1. Monitoring results on degraded beached plastic bags

In the 3 surveyed coastal sites of Syros Island, 327 plastic bags from super-markets and other retail shops were recorded and removed, of which 282 were shredded (86%). Most of the beach-stranded plastic bags were super-market/grocery shop bags (256 items; 78% of total plastic bags). The vast majority of the super-market/grocery shop plastic bags were shredded (89%). The thicker (>50 μm) retail-shop plastic bags were less abundant in the coastal sites (71 items; 22% of total plastic bags). Most of the retail shop bags were shredded (77%) as well, but not as much as the thinner (15–50 μm) supermarket bags. Oxo-degradable bags were scarce (5 items; 1.5%), and all of them were heavily shredded.

The biggest fluctuation in shredded plastic bag percentage, was observed in Ladopoulos Beach, especially after May 2018 (Fig. 1). Ladopoulos is an urban beach located within the premises of capital of the island, Ermoupolis. It is a heavily polluted beach, where litter is deposited by both wind-driven currents and on-site disposal. Litter in Ladopoulos Beach originates both from urban activities, due to the proximity to a densely populated area, but also from marine-based activities (i.e., navigation, fishery, etc.). It is the far most polluted site from the three that are included in this work; 195 (60%) of the plastic bags of this data set, were recorded in this beach. In Ladopoulos Beach, in August 2018, a much lower percentage of shredded super-market bags (47%), almost similar to the percentage of retail bags (39%) was recorded, resulting in a total 43% of shredded plastic bags. This may be attributed to the fact that since January 1st, 2018, thin (15–50 μm) plastic bag charges ("green" fee) were introduced by the Greek legislation in an effort to minimize their impact on the environment. Plastic bag thickness of 15–50 μm was the thickness traditionally used for super-market/grocery shop bags until then. As a result most Greek super-markets shifted to selling thicker plastic bags rather than giving away for free thin plastic bags to their customers, which was no longer an option. Hence, gradually the super-market/ bags found in the marine environment after the several months of the "green" plastic bag fee imposition, could be more resistant to degradation, since they have been produced to be thicker. Nevertheless, more plastic bag monitoring in the marine environment and comparison to earlier data is required to confirm this hypothesis.

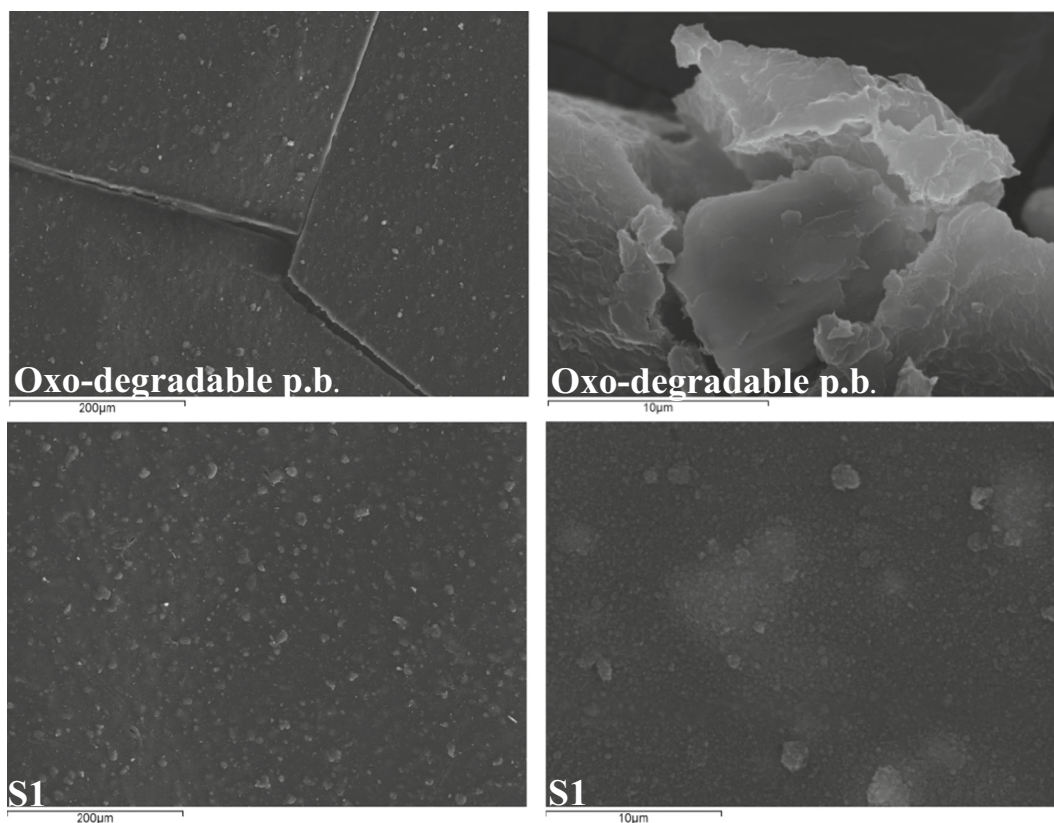


Fig. 2. SEM images of the plastic bags surfaces and a virgin LDPE (in two magnifications up to down): the oxo-degradable plastic bag (up), S1, S2, S3, S4, S5, S6 sample and a virgin LDPE (down).

Note that images S6 and Virgin LDPE on the left are in different magnification than the images on the left for the rest of the samples.

3.2. Surface characterization

Surface topographies obtained via SEM of all the plastic samples are illustrated in Fig. 2. Surface topography of a virgin LDPE was presented (smooth-glossy surface) at 100 (scale bar: 500 µm) and 5000× (scale bar: 10 µm). For oxo-degradable P.B., cracked areas in both magnifications were observed. For S1 plastic bag, smooth surface topography was observed in both magnifications (200 and 4000×) while for S2 (200 and 4000×) a rough (~abrasively) surface was determined. The surface topography of the S3 in both magnifications (200 and 6000×) (scale bar: 200 and 9 µm) was also smooth. Holes are observed throughout the smooth surface of S4 sample at 200× (scale bar: 200 µm) and were also observed in the 3000× (scale bar: 10 µm) image. Degradation of the surface (rough surface) was also observed in both magnifications (200 and 4000×) in the S5 sample. Cracked area is observed on the S6 surface in magnification 60× (scale bar: 900 µm) and smooth surface in magnification at 4000× (scale bar: 10 µm).

3.3. Identification of chemical bonds

Fig. 3 shows the Raman spectra for all the samples. According to the virgin LDPE spectrum the peaks observed at 1060 (C–C stretching) (Nauendorf et al., 2016), 1127 (C–C stretching) (Nauendorf et al., 2016), 1293 (CH₂ twisting) (Nauendorf et al., 2016), 1438 (CH₂ bending) (Nauendorf et al., 2016), 1747 (C = O ester carbonyl stretch mode) (Telle and Ureña, 2018), 2847 (symmetric CH₂ stretching mode)

(Ibrahim et al., 2017) and 2880 cm⁻¹ (asymmetric CH₂ stretching mode) (Ibrahim et al., 2017) are native to the polymer. These peaks disappear in the spectra S3 to S6 except the 1293, 2847, and 2880 cm⁻¹ in the S6 spectrum. On the other hand (the red arrows in S2 spectrum) 842 (symmetric of the SiO₄ group) (Paques-Ledent and Tarte, 1973), 2540 (SH stretching vibration) (Colthup et al., 1990), 2847 (symmetric CH₂ stretching mode) (Ibrahim et al., 2017) and 2881 cm⁻¹ (asymmetric CH₂ stretching mode) (Ibrahim et al., 2017) exist in the S1 spectrum and not in the oxo-degradable P.B. spectrum. The peaks at low wavenumbers suggest that the beached plastic bags retain sand/sediment on their surface even after they are well-wiped with a wet paper towel.

3.4. Identification of functional groups

According to the IR spectra (Figs. 4 and 5), two plastic groups were observed. Both S1 and S2 plastic bag samples were oxo-degradable plastic bags similar with (P.B.) (1st group) (Table 2) while S3, S4, S5, and S6 samples are similar with LDPE virgin sample (2nd group) (Table 3).

Five similar peaks at 2915, 2847, 1460, 875, and 718 cm⁻¹ were observed in the 1st group (Table 2). The peak at 1377 cm⁻¹ (1379 cm⁻¹ for the S2), did not exist at the oxo-degradable P.B. which correspond to methyl group based on literature (Jung et al., 2018). On the other hand, additional peaks due to degradation appeared in the oxo-degradable P. B. spectrum [2184, 2048, 1711 and 1413 cm⁻¹ which correspond to -N≡C stretch (Pillai, 2007), Berreman effect (Nalwa, 2001; Harbecke

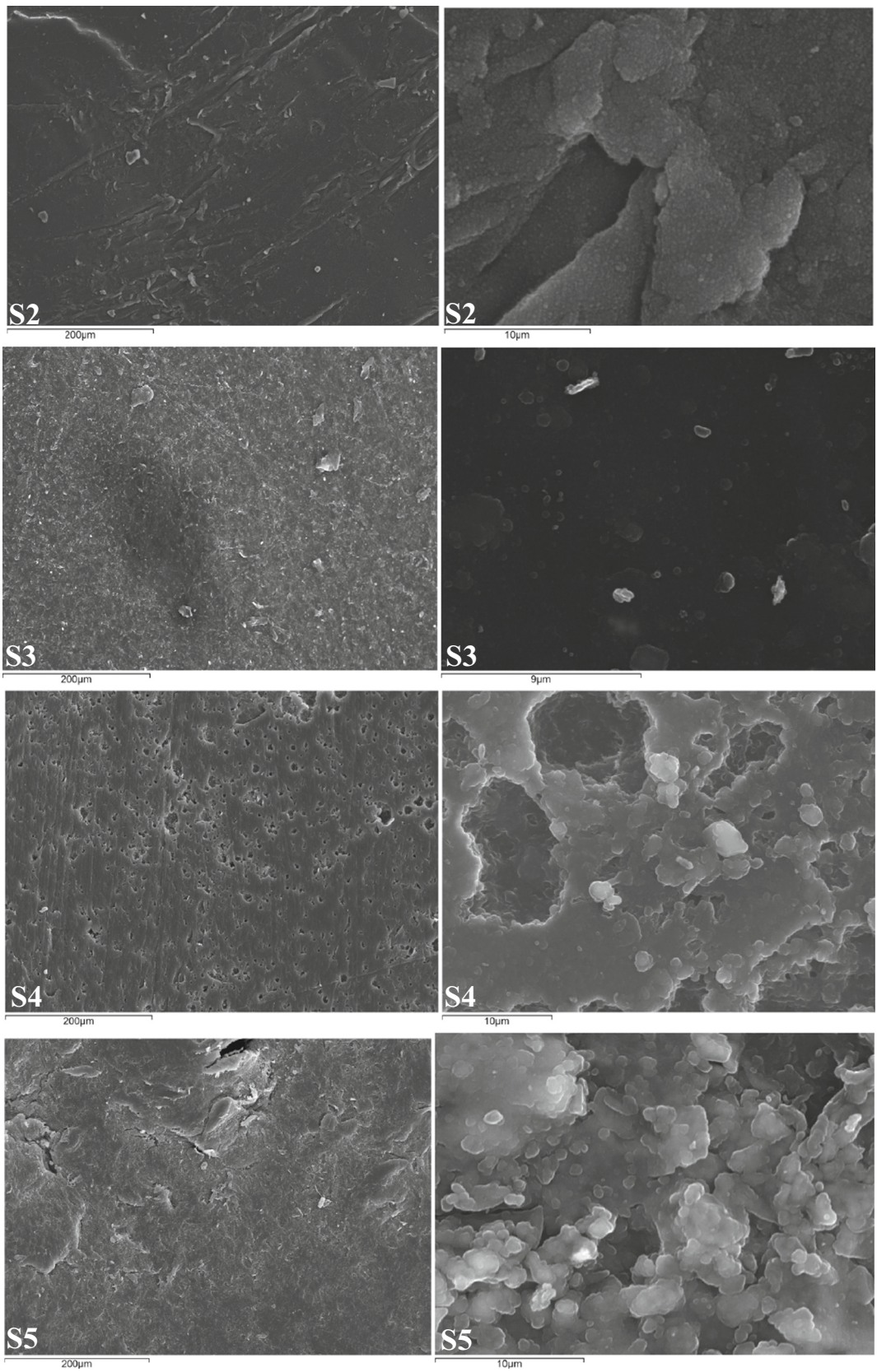


Fig. 2. (continued).

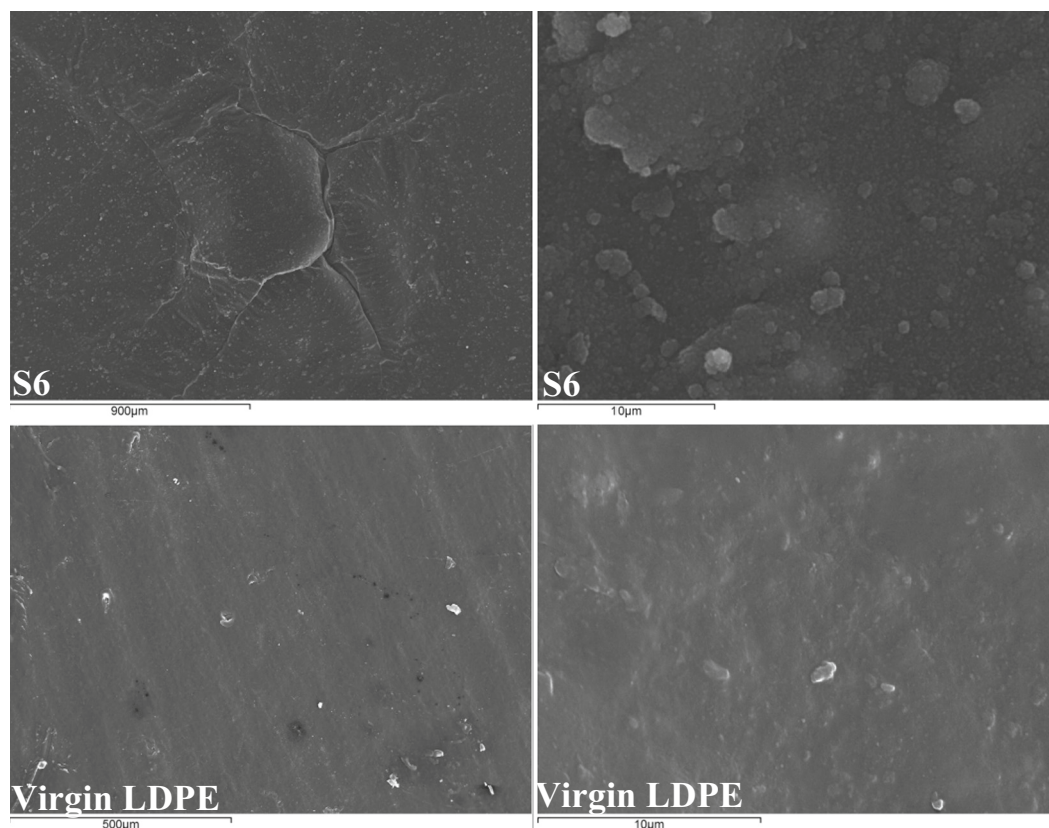


Fig. 2. (continued).

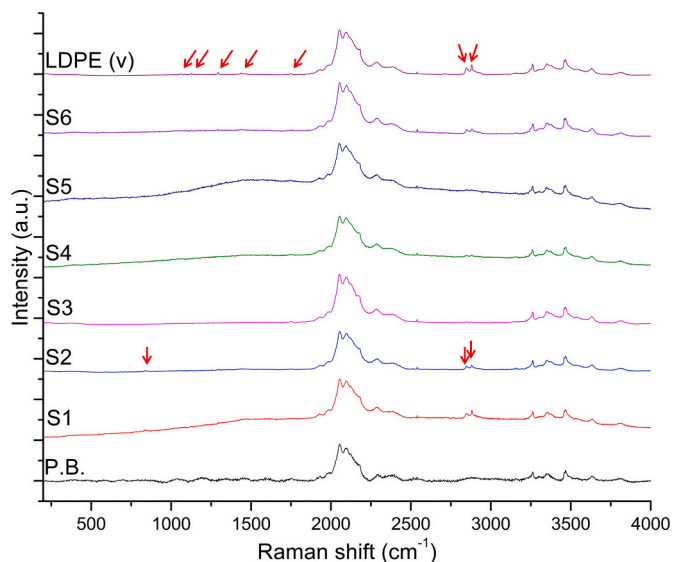


Fig. 3. Raman spectra of the plastic bag samples and a virgin LDPE.

et al., 1985), keto carbonyl bond (Musiol et al., 2017) and (possible) CH₂ symmetrical scissoring in Si-CH₂ (Fonceca et al., 1998), respectively]. Peaks at 428 (in S1), 514 and 418 cm⁻¹ (in oxo-degradable P.B.) correspond to feldspar (microcline), quartz and feldspar (albite) (Sivakumar et al., 2012), respectively; some of these peaks correspond to starch degradation 1413 cm⁻¹, (or/and 875 cm⁻¹) (Kizil et al., 2002),

1377 (S1), 1379 (S2) cm⁻¹ (Ashok et al., 2018) and 2184 cm⁻¹ (Orhan et al., 2004).

In the 2nd group, peak at 718 cm⁻¹ (CH₂ rock) in the LDPE virgin spectrum was observed to be displaced in S3, S4, S5 and S6 spectra (Table 3). Additional peaks due to environmental exposure were found in S3 to S6 samples. Peak at 1377 cm⁻¹ was observed in S3 (1379 cm⁻¹), S4 and S6 spectra that related with methyl group (Jung et al., 2018). Based on Fotopoulou and Karapanagioti (2015), the peak at 1034 cm⁻¹ was related on C-O-C (ester linkage) was detected on S4 (1036 cm⁻¹), S5, and S6. The peaks at 1470, 1409 (also in S4 at 1411 cm⁻¹) and 883 cm⁻¹ were found on S3 and correspond to CH₂ bend (Mitchell et al., 2013), CH₂ symmetrical scissoring in Si-CH₂ (Fonceca et al., 1998) and boron oxide (Beyli et al., 2008), respectively. The peak at 465 cm⁻¹ in S4 spectrum was detected also in S5 at 467 cm⁻¹ and corresponds to Si-O asymmetrical bending vibration (Sivakumar et al., 2012). 2162, 1368 and 528 cm⁻¹ were detected in S5 spectrum corresponding to Si-H stretching vibration (Jarosz et al., 2019), CH₂ wagging and/or symmetrical CH₃ movements (Fonceca et al., 1998) and feldspar (Sivakumar et al., 2012), respectively.

The carbonyl and vinyl indices of plastic bags can be calculated from FTIR results. Table 4 presents the ester, keto, and vinyl indices values of each sample (Kaberi et al., 2013; Fotopoulou and Karapanagioti, 2015). The virgin LDPE was used as a blank sample. The S6 had the lowest indices values of all samples, while the oxo-degradable P.B. the highest one. S5 ester, keto, and vinyl indices were estimated to be 0.11, 0.12, and 0.16 respectively, while S4 indices were at 0.19, 0.20, and 0.26, respectively. Finally, S1, S2, and S3 indices had similar values. In summary, from the lowest to the highest values the samples are as follows:

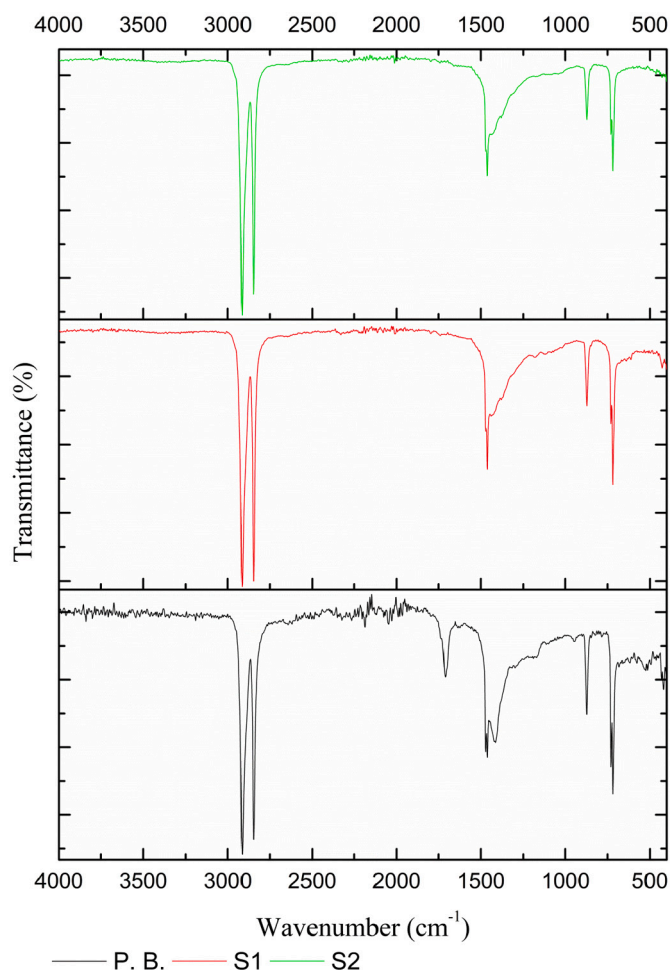


Fig. 4. ATR-IR spectra of the S1 (up), S2 (middle) and the oxo-degradable (P. B.) (down) plastic bags.

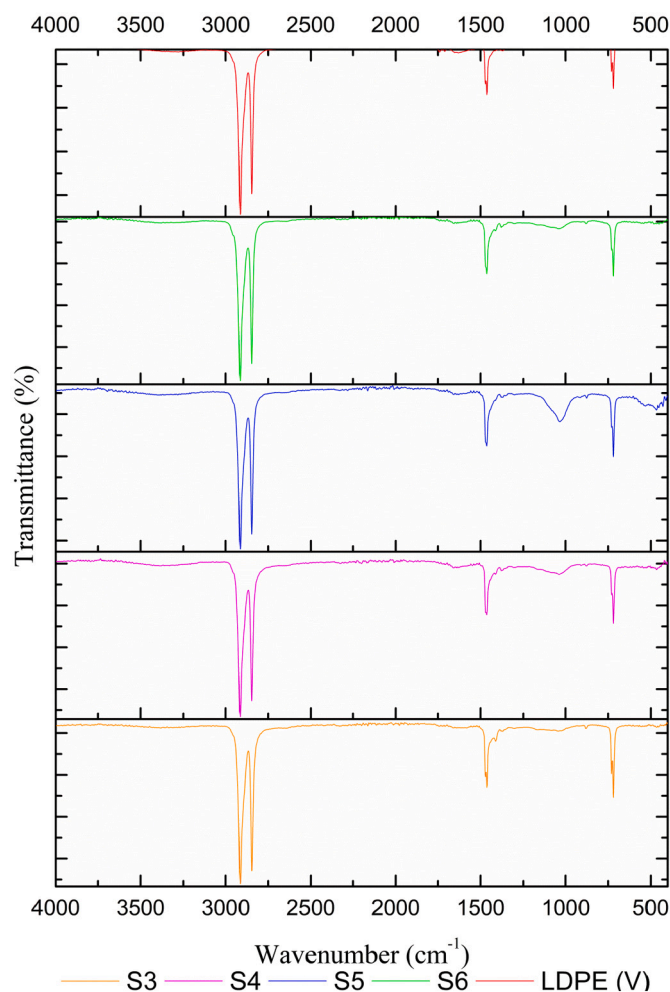


Fig. 5. ATR-IR spectra of the S3 (up), S4, S5, S6 and a virgin LDPE (down) plastics.

- Ester carbonyl index (I1715/I1465): oxo-degradable P.B. > S1, S2.
- Keto carbonyl index (I1740/I1465): oxo-degradable P.B. > S1, S2.
- Vinyl index (I1640/I1465): oxo-degradable P.B. > S2 > S1.
- Ester carbonyl index: S4 > S3, S5 > S6 > virgin LDPE.
- Keto carbonyl index: S4 > S5 > S3 > S6 > virgin LDPE.
- Vinyl index: S4 > S5 > S3 > S6 > virgin LDPE.

where I is the IR intensity at 1715, 1740, 1640, and 1465 cm^{-1} that corresponds to ketone, ester carbonyl, vinyl bond, and methylene bands, respectively (Albertsson et al., 1987).

According to DR normalized spectra (Fig. 6), a shoulder in visible region (400–700 nm) was observed in all the LDPE plastic bags (S3–S6). Similar slightly offset wavelength values were recorded in 300–400 nm (e.g., peaks at 307, 347 and 361 nm for S5) in all the samples. Finally, differences of the peaks in 200–300 nm seemed to be present (~ 247 nm for S3, S4 and S5/ ~ 230 nm for S4 and S5/ ~ 218 nm for S4 and S5/ ~ 214 nm for S6). This agrees with Rtimi et al. (2015) that observed the shift of the spectra towards smaller wavelengths due to degradation and the formation of oxygen functional groups. It was observed that C–O type functional groups, break H–C and C–C bonds and segment the PE film.

4. Discussion

Based on ATR-FTIR and Raman spectra, samples were grouped into two groups: a) oxo-degradable and b) LDPE. Macro- and micro- observations were correlated with the spectra. In both groups, additional peaks were observed in the beached samples due to environmental exposure, compared to the virgin samples which were not exposed to environmental conditions.

Oxo-degradable plastic bags use starch as adhesive of the synthetic polymer pieces (e.g., polyethylene) (Sandhu and Shakya, 2019); starch was characterized by ATR-FTIR spectra (Ashok et al., 2018). No significant differences in peaks can be observed in the S1 and S2 in contrast with the oxo-degradable plastic bag which was three years in a dark place in the air. This can also be observed macro- and microscopically, while in specific S2 seems to suffer from mechanical degradation (e.g., abrasion). Working in soil conditions with oxo-degradable plastic bags, Orhan et al. (2004) did not detect degradation of the synthetic polymer, while degradation of the starch added to the plastic was observed. A different study reported that oxo-biodegradable and conventional plastics degrade relatively slower than compostable plastics (O'Brine and Thompson, 2010).

Table 2

ATR-IR peaks of the S1, S2 and the oxo-degradable P.B. samples.

Samples	Main Peaks (cm ⁻¹)	Peaks based on literature	References
S1 & S2	2915 (S1), 2913 (S2)	2920 cm ⁻¹ stretching vibration of CH ₂ bonds.	Finzi-Quintão et al., 2016
	2847	2852 cm ⁻¹ stretching vibration of CH ₂ bonds.	Finzi-Quintão et al., 2016
	1460 (S1), 1462 (S2)	1462 cm ⁻¹ CH ₂ bending.	Fonceca et al., 1998
	1377 (S1), 1379 (S2)	1377 cm ⁻¹ methyl group.	Jung et al., 2018
	873	874 cm ⁻¹ amorphous phase of CH ₂ rock.	Finzi-Quintão et al., 2016
	730	726 cm ⁻¹ bending vibration absorption of CH-plane of the benzene ring bonds.	Finzi-Quintão et al., 2016
		727 cm ⁻¹ CH bonds.	
	718	720 cm ⁻¹ crystalline phase of CH ₂ rock.	Finzi-Quintão et al., 2016
	428 (S1)	428 cm ⁻¹ feldspar (microcline).	Sivakumar et al., 2012
	Oxo-degradable P.B.	2913	2920 cm ⁻¹ stretching vibration of CH ₂ bonds.
2845		2852 cm ⁻¹ stretching vibration of CH ₂ bonds.	Finzi-Quintão et al., 2016
2184		2180 cm ⁻¹ -N=C stretch.	Pillai, 2007
2048		2050 cm ⁻¹ Berreman effect.	Nalwa, 2001; Harbecke et al., 1985
1711		1717 cm ⁻¹ keto carbonyl bond.	Musiol et al., 2017
1460		1462 cm ⁻¹ CH ₂ scissoring vibration.	Musiol et al., 2017
1413		1415 cm ⁻¹ starch	Kizil et al., 2002
		1408 cm ⁻¹ CH ₂ symmetrical scissoring in Si-CH ₂ .	Fonceca et al., 1998
875		874 cm ⁻¹ amorphous phase of CH ₂ rock.	Finzi-Quintão et al., 2016
718		720 cm ⁻¹ crystalline phase of CH ₂ rock.	Finzi-Quintão et al., 2016
514	519 cm ⁻¹ quartz.	Sivakumar et al., 2012	
418	420 cm ⁻¹ feldspar (albite).	Sivakumar et al., 2012	

In the 2nd group (LDPE bags), S4 and S5 bags were presented to have more ATR-FTIR peaks than the S3 and S6, which agree macroscopically. At this point SEM images illustrated significant changes in the surfaces topography (S4 and S5). Different smaller holes and cracks were also observed by Napper and Thompson (2019) in a conventional bag (High Density Polyethylene). In addition, a cracked area on S6 with no significant additional peaks in its spectra was detected. This agrees with experiments performed with seawater by Alvarez-Zeferino et al. (2015) who found that plastic bags tend to fragment before significant chemical degradation was identified. Likewise, studying different types of plastic bags, exposed for 9 months in the open-air, Napper and Thompson (2019) observed that all bags were fragmented into particles; thereafter, the loss of tensile stress in conventional polyethylene, calculating 31% in open-air and 2% in the marine environment (Napper and Thompson, 2019). Experimenting with a number of plastics, Pegram and Andradý (1989) reported similar contrast in the rate of deterioration from the changes in tensile elongation at break between open-air (95%) and marine environment (2%). Finally, exposing polyethylene in the Baltic Sea in 2 m depth for 20 months, Rutkowska et al. (2002) did not observe any biodegradation.

Another interesting point is the formation of polar groups on the surface of these plastic bags. This makes the surface more hydrophilic and allows the interaction of the plastic surface with suspended solids, ions, and microbes (Fotopoulou and Karapanagioti, 2012, 2015; Holmes et al., 2012, 2014; Ashton et al., 2010). DRS technique was also used by

Table 3

ATR-IR peaks of the S3, S4, S5, S6 and a virgin LDPE plastic.

Samples	Main peaks (cm ⁻¹)	Peaks based on literature	References
Native peaks			
	2913	2915 cm ⁻¹ C-H stretch. 2900 cm ⁻¹ C-H ₂ asymmetrical stretch.	Jung et al., 2018 Fotopoulou and Karapanagioti, 2015
	2847	2845 cm ⁻¹ C-H stretch. 2850 cm ⁻¹ C-H ₂ symmetrical stretch.	Jung et al., 2018 Fotopoulou and Karapanagioti, 2015
LDPE (virgin)	1462	1462 cm ⁻¹ CH ₂ bend.	Jung et al., 2018
	1462	1464 cm ⁻¹ C-H ₂ bending.	Fotopoulou and Karapanagioti, 2015
	718	717 cm ⁻¹ CH ₂ rock. 720 cm ⁻¹ C-H ₂ rocking.	Jung et al., 2018 Fotopoulou and Karapanagioti, 2015
Additional peaks due to environmental exposure			
	1470	1470 cm ⁻¹ CH ₂ bend.	Mitchell et al., 2013
	1409	1408 cm ⁻¹ CH ₂ symmetrical scissoring in Si-CH ₂ .	Fonceca et al., 1998
S3	1379	1377 cm ⁻¹ methyl group.	Jung et al., 2018
	883	883 cm ⁻¹ .	Šeděnková, 2008
	730	883 cm ⁻¹ (boron oxide). 729 cm ⁻¹ CH ₂ rocking.	Beyli et al., 2008 Fonceca et al., 1998
	1411	1408 cm ⁻¹ CH ₂ symmetrical scissoring in Si-CH ₂ .	Fonceca et al., 1998
	1377	1377 cm ⁻¹ methyl group.	Jung et al., 2018
	1036	1040 cm ⁻¹ (C-O-C) ester linkage.	Fotopoulou and Karapanagioti, 2015
S4	877	874 cm ⁻¹ (CH ₂) rock amorphous.	Finzi-Quintão et al., 2016
	724	722 cm ⁻¹ CH ₂ rocking.	Fotopoulou and Karapanagioti, 2012
	465	459 cm ⁻¹ (Si-O) asymmetrical bending vibration.	Sivakumar et al., 2012
	2162	2165 cm ⁻¹ Si-H stretching vibration.	Jarosz et al., 2019
	1368	1366 cm ⁻¹ CH ₂ wagging and/or symmetrical CH ₃ movements.	Fonceca et al., 1998
	1034	1040 cm ⁻¹ (C-O-C) ester linkage.	Fotopoulou and Karapanagioti, 2015
S5	877	874 cm ⁻¹ (CH ₂) rock amorphous.	Finzi-Quintão et al., 2016
	728	729 cm ⁻¹ CH ₂ rocking.	Fonceca et al., 1998
	528	535 cm ⁻¹ feldspar. 459 cm ⁻¹ (Si-O)	Sivakumar et al., 2012
	467	asymmetrical bending vibration.	Sivakumar et al., 2012
	1411	1414 cm ⁻¹ asymmetric C-H bending.	González-Rivera et al., 2018
	1377	1377 cm ⁻¹ methyl group.	Jung et al., 2018
S6	1034	1040 cm ⁻¹ (C-O-C) ester linkage.	Fotopoulou and Karapanagioti, 2012
	877	874 cm ⁻¹ (CH ₂) rock amorphous.	Finzi-Quintão et al., 2016
	728	729 cm ⁻¹ (CH ₂) rocking.	Fonceca et al., 1998

Tziourrou et al. (2020) who have studied the interactions of LDPE – marine microbes; they observed also peaks in UV region at 200–220 nm ($n-\sigma^*$ and/or $\pi-\pi^*$) and 260–280 nm ($\pi-\pi^*$) electron transitions indicating organic functional groups and aromatic - polyaromatic compounds, respectively. Finally, there are $n-\pi^*$ electron transitions (260–280 nm) in most conjugated molecules (e.g., proteins and nucleic acids) (Bikova and Treimanis, 2004; Jia et al., 2007; Trabelsi et al., 2009; Rtimi et al., 2015). These interactions can cause the plastic bags to sink and this can explain their higher abundance in the bottom of the sea than on the beach where they tend to degrade and form microplastics.

Future investigations should pay attention to the type and of course to the shape (e.g., film) of sampling microplastics for a better description of their origin (e.g., plastic bags). The study of plastics in the

Table 4

Ester, keto, and vinyl indices found on all the samples. For the calculation of these indices the peaks at 1740, 1715, and 1640 cm^{-1} are divided with the peak at 1465 cm^{-1} that corresponds to the invariant absorbance of the $-\text{CH}_2-$ bond to calculate the ester, keto, and vinyl indices, respectively (Kaberi et al., 2013; Fotopoulou and Karapanagioti, 2015; Tziourrou et al., 2019).

Sample	Ester index	Keto index	Vinyl index
S1	0.11	0.10	0.12
S2	0.11	0.10	0.14
S3	0.11	0.10	0.13
S4	0.19	0.20	0.26
S5	0.11	0.12	0.16
S6	0.07	0.07	0.11
Oxo-degradable P.B.	0.29	0.52	0.23
LDPE (virgin)	0.05	0.04	0.07

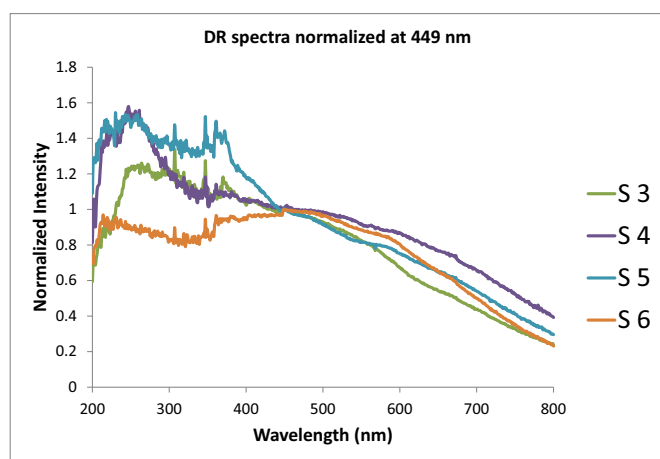


Fig. 6. DR normalized spectra for the LDPE plastic bags (S3–S6).

environment can be associated with mineralogy, as we encounter attached minerals on the plastic surface that could possibly provide insights on the transport and fate of plastics through different marine environments.

5. Conclusions

The main conclusion of the present study is that plastic bags can break into microplastics [see the abrasive surface in S2 (oxo-degradable material) and the irregular-cracked area in S6 (LDPE material)]. In the present study, three different ways of microplastic formation were observed (a) due to the presence of oxo-degradable substances such as starch added during the production, which is the adhesive of the synthetic polymer pieces in an oxo-degradable plastic bag; starch degradation was observed; no chemical alteration of the synthetic polymer was observed, (b) mechanical alterations take place leading to fragmentation, before major chemical modifications can be detected in synthetic polymers due to environmental exposure; this was visualized using SEM and observing holes and cracks in samples that did not show any chemical modification on their surface, and (c) oxidation of the surface due to chemical degradation; this was observed through spectroscopy techniques that found the formation of C—O type functional groups, leading to H—C and C—C bonds breakage and thus, segmentation of plastic bags.

Regulating the use of thin plastics bags not only lowers the number of plastic bags in the environment but also results in less fragmented bags and thus, less film-shaped microplastics. Considering that it is easier to manage macroplastics than microplastics the manufacturing process should be regulated to produce plastic bags that do not easily deteriorate to microplastics.

CRedit authorship contribution statement

P. Tziourrou: Investigation, Writing – original draft. **S. Kordella:** Investigation, Writing – original draft. **Y. Ardali:** Supervision. **G. Papatheodorou:** Funding acquisition, Supervision. **H.K. Karapanagioti:** Conceptualization, Writing – review & editing.

Declaration of competing interest

The authors declare that they have no known competing financial interests or personal relationships that could have appeared to influence the work reported in this paper.

Acknowledgments

The authors would like to thank:

- Professor Ioannis Kallitsis, Dr. Aikaterini K. Andreopoulou, and Aivali Stefania of the Advanced Polymers & Hybrid Nanomaterials Research Group of the Department of Chemistry of the University of Patras for the provision of ATR-FTIR spectrophotometer (Bruker) and helpful discussions.
- Professor Christos Kordulis and Dr. John Vakros of the Heterogeneous Catalysis Research Group of the Department of Chemistry of the University of Patras for the provision of the UV-Vis spectrophotometer (Varian Cary 3) and helpful discussions.
- Dr. Andreas Seferlis and Dr. Vayia Xanthopoulou of the Laboratory of Electron Microscopy and Microanalysis (L.E.M.M.) of University of Patras.

Funding information

This research was supported by:

- The General Secretariat for Research and Technology (GSRT) and Hellenic Foundation for Research and Innovation (HFRI) for Pavlos Tziourrou scholarship (12671).
- Beach litter fieldwork and study in Syros Island was carried out in the framework of LIFE DEBAG project (LIFE14 GIE/GR/001127) funded with the contribution of the European Union's LIFE financial instrument, the Green Fund, and Laboratory of Marine Geology and Physical Oceanography, Department of Geology, University of Patras own funds.

References

- Albertsson, A.C., Andersson, S.O., Karlsson, S., 1987. The mechanism of biodegradation of polyethylene. *Polym. Degrad. Stab.* 18, 73–87.
- Alvarez-Zeferino, J.C., Beltrán-Villavicencio, M., Vázquez-Morillas, A., 2015. Degradation of plastics in seawater in laboratory. *Open J. Polym. Chem.* 5, 55–62.
- Ashok, A., Abhijitha, R., Rejeesh, C.R., 2018. Material characterization of starch derived bio degradable plastics and its mechanical property estimation. *Mater. Today Proc.* 5, 2163–2170.
- Ashton, K., Holmes, L., Turner, A., 2010. Association of metals with plastic production pellets in the marine environment. *Mar. Pollut. Bull.* 60, 2050–2055.
- Balestri, E., Menicagli, V., Vallerini, F., Lardicci, C., 2017. Biodegradable plastic bags on the seafloor: a future threat for seagrass meadows? *Sci. Total Environ.* 605–606, 755–763.
- Beyli, P.T., Doğan, M., Gündüz, Z., Alkan, M., Turhan, Y., 2008. Synthesis, characterization and their antimicrobial activities of boron oxide/poly(acrylic acid) nanocomposites: thermal and antimicrobial properties. *Adv. Mater. Sci.* Vol. 18, No. 1 (55).
- Bikova, T., Treimanis, A., 2004. UV-absorbance of oxidized xylan and monocarboxyl cellulose in alkaline solutions. *Carbohydr. Polym.* 55, 315–322.
- Chiba, S., Saito, H., Fletcher, R., Yogi, T., Kayo, M., Miyagi, S., Ogido, M., Fujikura, K., 2018. Human footprint in the abyss: 30 year records of deep-sea plastic debris. *Mar. Policy* 96, 204–212.
- Clemente, C.C.C., Paresque, K., Santos, P.J.P., 2018. The effects of plastic bags presence on a macrobenthic community in a polluted estuary. *Mar. Pollut. Bull.* 135, 630–635.

- Colthup, N.B., Daly, L.H., Wiberley, S.E. 1990. Introduction to Infrared and Raman Spectroscopy. Third edition. Academic Press, INC. Harcourt Brace Jovanovich, Publishers. Printed in the United States of America.
- Digka, N., Tsangaris, C., Kaberi, H., Adamopoulou, A. and Zerl, C. 2018. Microplastic Abundance and Polymer Types in a Mediterranean Environment. Springer International Publishing AG. M. Cocca et al. (eds.), Proceedings of the International Conference on Microplastic Pollution in the Mediterranean Sea, Springer Water, http://doi.org/10.1007/978-3-319-71279-6_3.
- Eriksen, M., Lebreton, L.C.M., Carson, H.S., Thiel, M., Moore, C.J., Borerro, J.C., Galgani, F., Ryan, P.G., Reisser, J., 2014. Plastic pollution in the world's oceans: more than 5 trillion plastic pieces weighing over 250,000 tons afloat at sea. *PLoS ONE* 9 (12), e111913.
- Fenzi-Quintão, C.M., Novack, K.M., Bernardes-Silva, A.C., 2016. Identification of biodegradable and oxo-biodegradable plastic bags samples composition. *Macromol. Symp.* 367, 9–17.
- Fonceca, J.L.C., Barker, C.P., Badyal, J.P.S., 1998. Glow discharge oxidation of plasma polymerized organosilicon layers. In: First International Congress on Adhesion Science and Technology: Invited Papers. VSP, Utrecht, Netherlands, pp. 373–386.
- Fotopoulou, K., Karapanagioti, H.K., 2012. Surface properties of beached plastic pellets. *Mar. Environ. Res.* 81, 70–77.
- Fotopoulou, K., Karapanagioti, H.K., 2015. Surface properties of beached plastics. *Environ. Sci. Pollut. Res.* 22, 11022–11032.
- Galgani, F., Hanke, G., Werner, S., Oosterbaan, L., Nilsson, P., Fleet, D., Kinsey, S., Thompson, R.C., Van Franeker, J., Vlachogianni, T., Scoullou, M., Mira Veiga, J., Palatinus, A., Matiddi, M., Maes, T., Korpinen, S., Budziak, A., Leslie, H., Gago, J., Liebbezeit, G., 2013. Guidance on Monitoring of Marine Litter in European Seas. MSFD Technical Subgroup on Marine Litter (TSG-ML).
- González-Rivera, J., Iglío, R., Barillaro, G., Duce, C., Tinè, M.R., 2018. Structural and thermoanalytical characterization of 3D porous PDMS foam materials: the effect of impurities derived from a sugar templating process. *Polymers* 10, 616.
- Green, D.S., Boots, B., Blockley, D.J., Rocha, C., Thompson, R., 2015. Impacts of discarded plastic bags on marine assemblages and ecosystem functioning. *Environ. Sci. Technol.* 49, 5380–5389.
- Harbecke, B., Heinz, B., Grosse, P., 1985. Optical Properties of Thin Films and the Berreman Effect. *Appl. Phys. A* 38, 263–267.
- Holmes, L.A., Turner, A., Thompson, R.C., 2012. Adsorption of trace metals to plastic resin pellets in the marine environment. *Environ. Pollut.* 160, 42–48.
- Holmes, L.A., Turner, A., Thompson, R.C., 2014. Interactions between trace metals and plastic production pellets under estuarine conditions. *Mar. Chem.* 167, 25–32.
- Ibrahim, M., He, H. and Thermo Fisher Scientific. 2017. Classification of polyethylene by Raman spectroscopy. ThermoScientific. APPLICATION NOTE AN52301. Available at: <https://assets.thermofisher.com/TFS-Assets/MSD/Application-Notes/AN52301-classification-polyethylene-Raman-spectroscopy-app-note.pdf>.
- J R C (Joint Research Centre), 2013. Guidance on monitoring of marine litter in European seas. In: Scientific and Policy Reports. <https://doi.org/10.2788/99475>.
- Jarosz, T., Kepska, K., Ledwon, P., Procek, M., Domagala, W., Stolarczyk, A., 2019. Poly (3-hexylthiophene) grafting and molecular dilution: study of a class of conjugated graft copolymers. *Polymers* 11, 205.
- Jia, S., Yu, H., Lin, Y., Dai, Y., 2007. Characterization of extracellular polysaccharides from *Nostoc flagelliforme* cells in liquid suspension culture. *Biotechnol. Bioprocess Eng.* 12, 271–275.
- Jung, M.R., Horgen, F.D., Orski, S.V., Rodriguez, C.V., Beers, K.L., Balazs, G.H., Jones, T. T., Work, T.M., Brigna, K.C., Royer, S.-J., Hyrenbach, K.D., Jensen, B.A., Lynch, J.M., 2018. Validation of ATR FT-IR to identify polymers of plastic marine debris, including those ingested by marine organisms. *Mar. Pollut. Bull.* 127, 704–716.
- Kaberi, H., Tsangaris, C., Zerl, C., Mousdis, G., Papadopoulos, A., Streftaris, N., 2013. Microplastics along the shoreline of a Greek island (Kea isl., Aegean Sea): types and densities in relation to beach orientation, characteristics and proximity to sources. In: 4th International Conference on Environmental Management, Engineering, Planning and Economics (CEMEPE) and SECOTOX Conference, pp. 197–202. Mykonos Island, 24–28 June 2013. Greece.
- Kalogerakis, N., Karkanorachaki, K., Kalogerakis, G.C., Triantafyllidi, E.I., Gotsis, A.D., Partsiavelos, P., Fava, F., 2017. Microplastics generation: onset of fragmentation of polyethylene films in marine environment mesocosms. *Front. Mar. Sci.* 4, 84.
- Kizil, R., Irudayaraj, J., Seetharaman, K., 2002. Characterization of irradiated starches by using FT-Raman and FTIR spectroscopy. *J. Agric. Food Chem.* 50 (3912 – 391).
- Knoblauch, D., Mederake, L., Stein, U., 2018. Developing countries in the lead-what drives the diffusion of plastic bag policies? *Sustainability* 10, 1994.
- Maes, T., Barry, J., Leslie, H.A., Vethaak, A.D., Nicolaus, E.E.M., Law, R.J., Lyons, B.P., Martinez, R., Harley, B., Thain, J.E., 2018. Below the surface: twenty-five years of seafloor litter monitoring in coastal seas of North West Europe (1992–2017). *Sci. Total Environ.* 630, 790–798.
- Masura, J., Baker, J., Foster, G. and Arthur, C. 2015. Laboratory Methods for the Analysis of Microplastics in the Marine Environment. NOAA Marine Debris Program, National Oceanic and Atmospheric Administration, U.S. Department of Commerce, Technical Memorandum NOS-OR&R-48.
- Mitchell, G., France, F., Nordon, A., Tang, P.L., Gibson, L.T., 2013. Assessment of historical polymers using attenuated total reflectance-Fourier transform infrared spectroscopy with principal component analysis. *Herit. Sci.* 1, 28.
- Moharam, R., Almaqtari, M.A., 2014. The impact of plastic bags on the environment: a field survey of the city of Sana'a and the surrounding areas, Yemen. *Int. J. Eng. Res. Rev.* 2 (4), 61–69.
- Musioli, M., Ryzd, J., Janeczek, H., Radecka, I., Jiang, G., Kowalczyk, M., 2017. Forensic engineering of advanced polymeric materials Part IV: Case study of oxo-biodegradable polyethylene commercial bag – Aging in biotic and abiotic environment. *Waste Management* 64, 20–27.
- Nalwa, H.S. 2001. Silicon-based Material and Devices. Properties and Devices. Hari Singh Nalwa. vol. 1. Academic Press.
- Napper, I.E., Thompson, R.C., 2019. Environmental deterioration of biodegradable, oxo-biodegradable, compostable, and conventional plastic carrier bags in the sea, soil, and open-air over a 3-year period. *Environ. Sci. Technol.* 53, 4775–4783.
- Nauendorf, A., Krause, S., Bigalke, N.K., Gorb, E.V., Gorb, S.N., Haeckel, M., Wahl, M., Treude, T., 2016. Microbial colonization and degradation of polyethylene and biodegradable plastic bags in temperate fine-grained organic-rich marine sediments. *Mar. Pollut. Bull.* 103, 168–178.
- O'Brine, T., Thompson, R.C., 2010. Degradation of plastic carrier bags in the marine environment. *Mar. Pollut. Bull.* 60, 2279–2283.
- Orhan, Y., Hrenović, J., Büyükgüngözü, H., 2004. Biodegradation of plastic compost bags under controlled soil conditions. *Acta Chim. Slov.* 51, 579–588.
- Paques-Ledent, M.T.H., Tarte, P., 1973. Vibrational studies of olivine-type compounds-I. The i.r. and Raman spectra of the isotopic species of Mg₂SiO₄. *Spectrochim. Acta* 29A, 1007–1016.
- Pegram, J.E., Andrady, A.L., 1989. Outdoor weathering of selected polymeric materials under marine exposure conditions. *Polym. Degrad. Stab.* 26 (4), 333–345.
- Pillai, K., 2007. FTIR-ATR Characterization of Hydrogel, Polymer Films, Protein Immobilization and Benzotriazole Adsorption on Copper Surface. Thesis prepared for the degree of Master of Science. University of North Texas.
- Rtimi, S., Pulgarin, C., Sanjines, R., Kiwi, J., 2015. Novel FeOx-polyethylene transparent films: synthesis and mechanism of surface regeneration. *R Soc Chem. RSC Adv.* 5, 80203–80211.
- Rummel, C.D., Jahnke, A., Gorokhova, E., Kühnel, D., Schmitt-Jansen, M., 2017. Impacts of biofilm formation on the fate and potential effects of microplastic in the aquatic environment. *Environ. Sci. Technol. Lett.* 4, 258–267.
- Rutkowska, M., Heimowska, A., Krasowska, K., Janik, H., 2002. Biodegradability of polyethylene starch blends in sea water. *Pol. J. Environ. Stud.* 11 (3), 267–274.
- Saidan, M.N., Ansour, L.M., Saidan, H., 2017. Management of plastic bags waste: an assessment of scenarios in Jordan. *J. Chem. Technol. Metall.* 52 (1), 148–154.
- Sandhu, R.S., Shakya, M., 2019. Comparative study of synthetic plastics and biodegradable plastics. *Glob. J. Bio-Sci. Biotechnol.* 8 (1), 107–112.
- Šeděnková, I., 2008. Spectroscopy of Conducting Polymers Thin Films. Dissertation thesis. Faculty of Mathematics and Physics. Charles University in Prague, Czech Republic.
- Shruti, V.C., Jonathan, M.P., Rodriguez-Espinosa, P.F., Rodríguez-González, F., 2019. Microplastics in freshwater sediments of Atoyac River basin, Puebla City, Mexico. *Sci. Total Environ.* 654, 154–163.
- Sivakumar, S., Ravisankar, R., Raghun, Y., Chandrasekaran, A., Chandramohan, J., 2012. FTIR spectroscopic studies on coastal sediment samples from Cuddalore District, Tamilnadu, India. *Indian J. Adv. Chem. Sci.* 1, 40–46.
- Telle, H.H. and Ureña, Á.G. 2018. Laser spectroscopy and laser imaging. An introduction. *Raman Spectroscopy in Liquid Samples* p. 323. CRC Press. Taylor and Francis Group.
- Trabelsi, L., Msakni, N.H., Ouada, H.B., Bacha, H., Roudesli, S., 2009. Partial characterization of extracellular polysaccharides produced by cyanobacterium *Arthrospira platensis*. *Biotechnol. Bioprocess Eng.* 14, 27–31.
- Tziourrou, P., Megalovasilis, P., Tsounia, M., Karapanagioti, H.K., 2019. Characteristics of microplastics on two beaches affected by different land uses in Salamina Island in Saronikos Gulf, east Mediterranean. *Mar. Pollut. Bull.* 149, 110531.
- Tziourrou, P., Vakros, J., Karapanagioti, H.K., 2020. Using diffuse reflectance spectroscopy (DRS) technique for studying biofilm formation on LDPE and PET surfaces: laboratory and field experiments. *Environ. Sci. Pollut. Res.* <https://doi.org/10.1007/s11356-020-07729-0>.
- Viršek, M.K., Palatinus, A., Koren, Š., Peterlin, M., Horvat, P., Kržan, A., 2016. Protocol for microplastics sampling on the sea surface and sample analysis. *J. Vis. Exp.* 118, e55161.
- Wessel, C.C., Lockridge, G.R., Battiste, D., Cebrian, J., 2016. Abundance and characteristics of microplastics in beach sediments: insights into microplastic accumulation in northern Gulf of Mexico estuaries. *Mar. Pollut. Bull.* 109, 178–183.
- Zhang, H., 2017. Transport of microplastics in coastal seas. *Estuar. Coast. Shelf Sci.* 199, 74–86.